

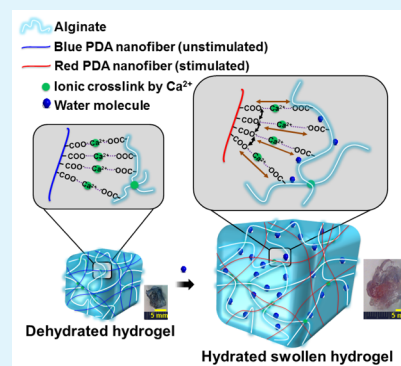
# Stimuli-Responsive Matrix-Assisted Colorimetric Water Indicator of Polydiacetylene Nanofibers

Sungbaek Seo,<sup>†,∇,#</sup> Jiseok Lee,<sup>†,○,#</sup> Min Sang Kwon,<sup>‡</sup> Deokwon Seo,<sup>‡</sup> and Jinsang Kim<sup>\*,†,‡,§,||,⊥</sup>

<sup>†</sup>Macromolecular Science and Engineering, <sup>‡</sup>Materials Science and Engineering, <sup>§</sup>Chemistry, <sup>||</sup>Chemical Engineering, and <sup>⊥</sup>Biomedical Engineering, University of Michigan, Ann Arbor, Michigan 48109, United States

**ABSTRACT:** An alternative signal transduction mechanism of polydiacetylene (PDA) sensors is devised by combining stimuli-responsive polymer hydrogel as a matrix and PDA sensory materials as a signal-generating component. We hypothesized that volumetric expansion of the polymer hydrogel matrix by means of external stimuli can impose stress on the imbedded PDA materials, generating a sensory signal. PDA assembly as a sensory component was ionically linked with the alginate hydrogel in order to transfer the volumetric expansion force of alginate hydrogel efficiently to the sensory PDA molecules. Under the same swelling ratio of alginate hydrogel, alginate gel having embedded 1-dimensional thin PDA nanofibers (~20 nm diameter) presented a sharp color change while 0-dimensional PDA liposome did not give any sensory signal when it was integrated in alginate gel. The results implied that dimensionality is an important design factor to realize stimuli-responsive matrix-driven colorimetric PDA sensory systems; more effective contact points between 1-dimensional PDA nanofibers and the alginate matrix much more effectively transfer the external stress exerted by the volumetric expansion force, and thin PDA nanofibers respond more sensitively to the stress.

**KEYWORDS:** polydiacetylene, alginate hydrogel, volumetric expansion, nanofibers, water indicator



## INTRODUCTION

Physical properties and stability of polymeric hydrogel materials are readily tunable in aqueous media,<sup>1</sup> which together with their achievable biocompatibility make them an attractive platform for biomedical applications such as tissue engineering,<sup>2</sup> drug delivery,<sup>3</sup> wound healing,<sup>4</sup> and biosensors.<sup>5</sup> The open structure with large internal volume of polymeric hydrogels allows facile capturing of chemical and/or biological analytes. Stimuli-responsive polymer hydrogels have shown reversible swelling–shrinking behavior in response to various external stimuli such as temperature,<sup>6</sup> pH,<sup>7</sup> ionic strength,<sup>8</sup> light,<sup>9</sup> electric field,<sup>10</sup> and bioanalytes.<sup>11</sup>

Polymer hydrogels can also accommodate sensory nanomaterials, creating advanced composite materials to satisfy the demands of novel biosensor systems such as flexible electronics<sup>12–14</sup> and implantable medical devices.<sup>15–17</sup> For example, Zhai et al. developed an amperometric glucose sensor using polyaniline based hydrogel having excellent flexibility and conductivity as biosensor electrodes.<sup>18</sup> Grigoryev et al. fabricated electroconductive carbon nanotube embedded alginate hydrogel fibers for humidity and pH sensing, which enabled conversion of the swelling–shrinking behavior of the hydrogel into an electrical sensory signal<sup>19</sup> because the fiber conductivity was altered depending on the swelling of the hydrogel fiber. Under the humid and basic conditions, the fiber hydrogel expanded and lowered the number of contact points between the embedded carbon nanotubes. Accordingly, the fiber conductivity decreased as the hydrogel swelled. While electroconductive hydrogel sensors have been extensively

investigated, optical biosensors devised from polymer hydrogel or hydrogel-like platforms<sup>20–22</sup> are few. Since there is great potential of direct, real-time, and label-free detection of chemical and biological analytes without using any equipment, optical detection is a convenient and useful strategy.

Polydiacetylene (PDA) is a self-signalizing polymer exhibiting color changes from blue to red upon exposure to external stimuli, including temperature,<sup>23,24</sup> pH,<sup>25,26</sup> mechanical stress,<sup>27,28</sup> and chemical/biological analytes.<sup>29–39</sup> The signal transduction mechanism of PDA is believed to be based on the distortion of the self-assembled and photopolymerized conjugated yne-ene backbone of PDA by external stimuli. In particular, as for the chemical and biological analytes, steric repulsion at the surface of self-assembled PDA liposomes induced by specific receptor–target complex formation causes signal generation.<sup>29–34</sup> In this regard, in order to generate the sensory signal, adjacent receptors should be occupied by target molecules so that efficient repulsion between the receptor–target complexes should be realized. This condition can be satisfied only when a decent amount of analytes are available to capture, lowering the detection limit of the PDA sensory system.

Two-component sensory films based on composites of PDA in a polymer matrix have been reported.<sup>40–42</sup> In those examples, distinct solubility of a matrix polymer toward a target

Received: July 6, 2015

Accepted: August 21, 2015

Published: August 24, 2015

solvent allows selective dissolution of the embedded PDA, which generates a selective optical sensory signal. Herein, we demonstrated another signal transduction mechanism of PDA sensors by conjoining stimuli-responsive polymer hydrogel as a matrix and PDA sensory materials as a signal-generating constituent. We hypothesized that volumetric expansion of the polymer hydrogel matrix by means of external stimuli can impose stress on the imbedded PDA materials, generating a sensory signal. To investigate such a system design, we chose to develop a water indicator because water allows the hydrogel matrix to be responsive, e.g., to swell, to stress on the bound PDA materials. Since water cannot dissolve embedded PDA self-assemblies (i.e., no chances of generating optical sensory signal), we can investigate exclusively the matrix-induced signal generation possibility. In order to efficiently transfer the stress generated by a volume change of the hydrogel matrix to the sensory PDA component, we devised 1-dimensional PDA microcrystals, PDA nanofibers having different diameters, as well as conventional PDA liposomes, and we systematically investigated the effects of dimensionality on the sensory signal generation efficiency.

## EXPERIMENTAL SECTION

**Materials and Methods.** All solvents were purchased from Sigma-Aldrich. 10,12-pentacosadiynoic acid (PCDA) was purchased from GFS Chemicals. Oxalyl chloride and sodium alginate were obtained from Acros Organics. 5-Aminoisophthalic acid, lithium hydroxide, sodium hydroxide, potassium hydroxide, and calcium chloride were purchased from Sigma-Aldrich.

The synthesis of PCDA derivatives was described in the literature.<sup>43</sup> The PDA monomers were characterized with <sup>1</sup>H NMR spectra (500 MHz) using a Varian Inova 500 instrument. The morphology of the PDA assembly structures was observed with scanning electron microscopy images using an FEI Nova NanoLab instrument. The size and surface charge of the PDA liposome solution were measured by Malvern Zetasizer Nano-ZS. A hand-held UV lamp (254 nm, 1 mW cm<sup>-2</sup>, 2 min) was used for photopolymerization of PDA hydrogel. Photographs were taken using Sony NEX-F3 camera. Powder XRD patterns were measured by a Rigaku rotating anode X-ray diffractometer. UV-vis absorption spectra were obtained by Varian Cary 50 UV-vis spectrophotometer.

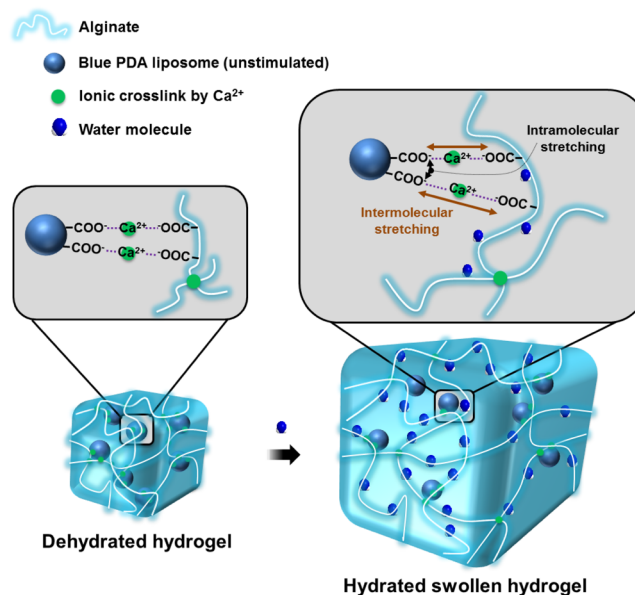
**Preparation of PDA liposome solution.** PDA liposome solution was prepared by the injection method; PCDA (3.7 mg) or PCDA-isophthalic acid (PCDA-IPA, 5.4 mg) were dissolved in 0.3 mL of tetrahydrofuran (THF), then the homogeneous THF solution was injected into a 20 mL of deionized water and subsequently dispersed in a probe sonicator for 10 min to produce the final concentration of 0.5 mM liposome. After filtration through a 0.8 μm cellulose acetate syringe filter, the resulting PDA liposome solution was stored at 5 °C at least 2 h.

**Preparation of PCDA microcrystals and PCDA-IPA nanofibers.** PCDA microcrystal was fabricated according to the literature.<sup>44</sup> To a 10 mL of 4 mM NaOH aqueous solution, 1.52 mg of purified colorless PCDA was added. The mixture solution was heated up to 90 °C with stirring to reach a clear homogeneous solution. The clear solution was cooled down to 5 °C and stored at the same temperature for 2 h. Sodium PCDA (PCDA-Na<sup>+</sup>) microcrystals then began to precipitate from the solution.

Likewise, to a 15 mL of 1 mM of alkali hydroxides (KOH or LiOH) solution, the purified colorless PCDA-IPA was added. The mixture solution was heated to 90 °C with stirring to produce a transparent solution. The solution was cooled down to 5 °C and stored overnight, then viscous potassium PCDA-IPA (PCDA-IPA-K<sup>+</sup>) and lithium PCDA-IPA (PCDA-IPA-Li<sup>+</sup>) nanofibers formation was observed in the solutions.

**Preparation of alginate hydrogel having embedded PDA assembly.** 4.7 mL of 0.5 mM PDA assemblies (liposomes or

### (a) PDA liposome embedded hydrogel



### (b) PDA nanofiber embedded hydrogel

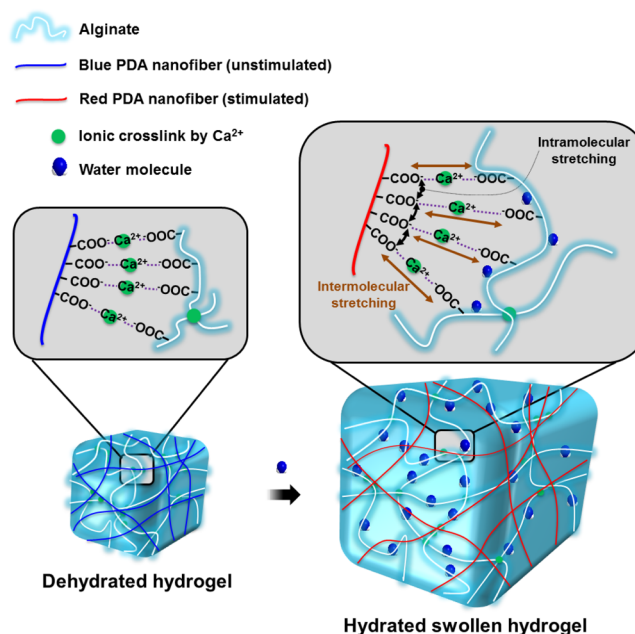


**Figure 1.** Proposed scheme of hydrogel assisted PDA mechanochromism. Unstimulated blue colored (a) PDA liposome (or (b) nanofiber) is cross-linked by divalent Ca<sup>2+</sup> with anionic alginate at a dehydrated stage. Once the hydrogel is swollen by hydration, the PDA liposome (or nanofiber) turns red, depending on how much the PDA liposome (or nanofiber) gets stressed (intermolecular stretching between PDA liposome (or nanofiber) and the alginate, plus intramolecular stretching in PDA liposome (or nanofiber)).

microcrystals or nanofibers) were homogeneously stirred with 4.7 mL of 4 wt % alginate solution in a 20 mL vial. To the mixture solution, 0.6 mL of 2 wt % calcium chloride solution was added to generate cross-linked gel with 30 min stirring. The gel was rinsed with deionized water 3 times to remove unreacted calcium chloride and subsequently dried in an oven at 40 °C.

#### Optimization of swelling condition for alginate hydrogels.

To a series of 9.4 mL alginate solutions (1, 2, 3, 4 wt %) in a 20 mL vial, 0.6 mL of calcium chloride (1, 2, 3, 4 wt %) solution was added to generate cross-linked gel with 30 min stirring. The gel was rinsed with

deionized water 3 times to remove unreacted calcium chloride and subsequently dried in an oven at 40 °C.

**Characterization of hydrogel swelling.** The dried hydrogels were weighed as dried state ( $W_d$ ). The dried hydrogels were immersed in 1 mL of deionized water for 1 h. The hydrogels were taken out and were blotted with a paper towel to remove excess water on their surface. Then, the swollen hydrogels were weighed as swollen state ( $W_s$ ). The swelling ratio ( $Q_s$ ) of test samples was calculated from the following equation.<sup>45</sup>

$$Q_s = (W_s - W_d)/W_d$$

The condition (concentration of alginate solution and calcium chloride solution) that caused the largest swelling was used for PDA chromism studies by hydrogel swelling.

**UV–vis absorption measurement and colorimetric response.** The dehydrated (or swollen) hydrogel was fixed on a transparent glass slide, placed perpendicular to the beam, and the absorption spectrum was obtained. Instrument baseline was measured before fixing the gel samples. Five different positions of each sample were scanned. Colorimetric responses (CR) of the hydrogel composite before and after water uptake were calculated by the well-known equation.<sup>46</sup> Here, the blue percentage (PB) is defined as  $PB = A_{\text{blue}} / (A_{\text{blue}} + A_{\text{red}}) \times 100\%$  where  $A_{\text{blue}}$  is the absorbance at the peak around 675 nm and  $A_{\text{red}}$  is the absorbance at the peak around 550 nm. Then, the CR is defined as  $CR = (\text{initial PB} - \text{final PB}) / \text{initial PB} \times 100\%$ .

## RESULTS AND DISCUSSION

We systematically investigated matrix polymer assisted PDA chromism in order to devise a sensitive hydrogel-based hybrid sensory system. First, we self-assembled PDA into liposome that

is the most common self-assembled structure of diacetylenes (DAs). As the polymer matrix we used alginate, a sodium salt of alginic acid, that is an anionic linear polymer and highly hygroscopic to absorb 200–300 times its own weight of water.<sup>47</sup> Due to the anionic character, alginate can be ionically cross-linked with divalent cations.<sup>45</sup> In order to convey external stimuli directly to the sensory PDA materials, we proposed to ionically cross-link the anionic PDA assembly together with the anionic alginate matrix using divalent cationic cross-linkers to form a hydrogel composite (Figure 1). To explain how the composite system works to detect water, in the magnified drawings of Figure 1, we illustrated a simplified model of cross-links and potential interactions. Figure 1a depicts ionic cross-links between a PDA liposome and an alginate fiber via  $\text{Ca}^{2+}$ , and a cross-link between alginate and alginate. Considering the size (~100 nm diameter) of the PDA liposome, it likely cross-links with only one alginate fiber while a much longer PDA nanofiber would form cross-linking with multiple alginate fibers (Figure 1b). Therefore, upon hydration of dried hydrogel, volumetric expansion between cross-links is anticipated to exert a stretching force much more effectively on PDA nanofiber than PDA liposome.

10,12-Pentacosadiynoic acid (PCDA) and PCDA-isophthalic acid (PCDA-IPA) are DA monomers and self-assemble to generally a liposome in aqueous medium due to their amphiphilic property. We developed a self-assembly protocol to make nearly 1-dimensional PDA microcrystals and nanofibers rather than conventional liposome by adapting a literature

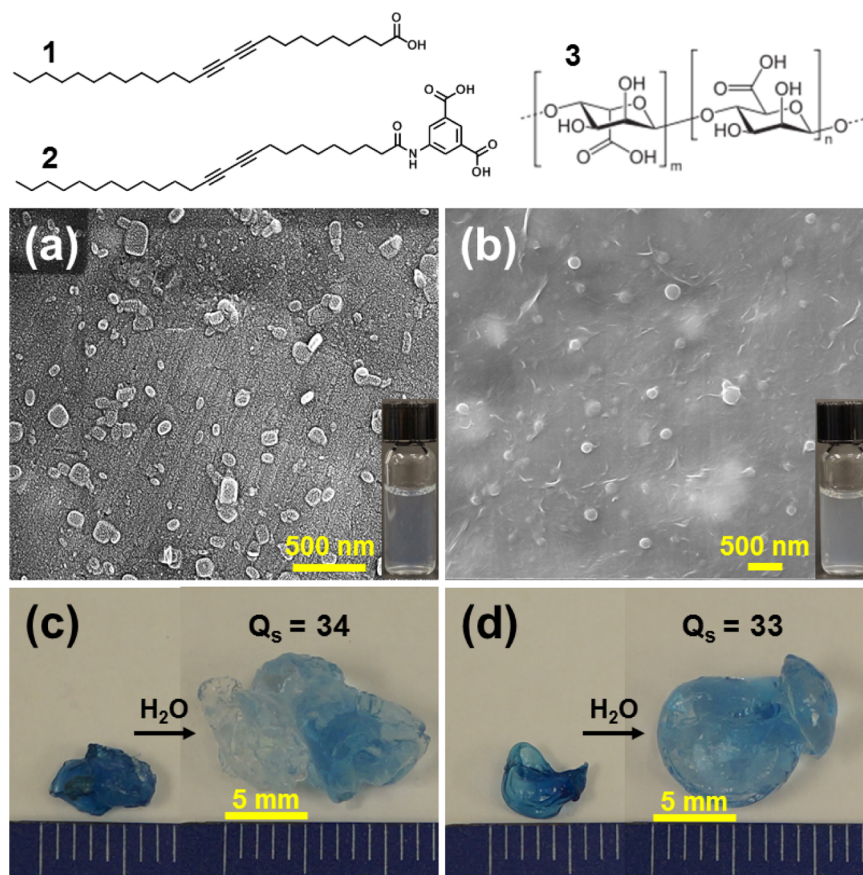


**Figure 2.** Chemical structures of PCDA (1), PCDA-IPA (2), and alginate (3). SEM images of (a) PCDA liposome and (b) PCDA-IPA liposome. Photograph of photopolymerized/dehydrated alginate hydrogel and hydrated hydrogel embedded with (c) PCDA liposome and (d) PCDA-IPA liposome.

method using alkali metal ions.<sup>44</sup> Through the developed protocols we could formulate 1-dimensional microcrystals, nanofibers, as well as liposomes of PCDA and PCDA-IPA, respectively.

We prepared PDA liposomes suspended in deionized water (inset of Figure 2a, b). Dynamic light scattering measurement revealed that the mean diameter of PCDA and PCDA-IPA liposomes is  $150 \pm 19$  nm and  $244 \pm 37$  nm, respectively. In the SEM images (Figure 2a, b), the spherical liposomes were observed and the diameters were consistent with the values from the light scattering measurement. In the PCDA-IPA suspension, bundles of fibers looked to coexist with liposomes, which is attributed to the intrinsic nature of both self-assemblies (Figure 2b). The surface charges of PCDA and PCDA-IPA liposomes are  $-34.6 \pm 10.6$  mV and  $-56.4 \pm 8.57$  mV, respectively, due to the carboxylic acid groups at the terminal of the DA. The anionic surface of the assembled DAs further enables ionic cross-linking of the liposomes with multivalent cations such as  $\text{Ca}^{2+}$ .

First, we optimized the concentration of alginate and calcium chloride ( $\text{CaCl}_2$ ) solution, respectively, in order to achieve the

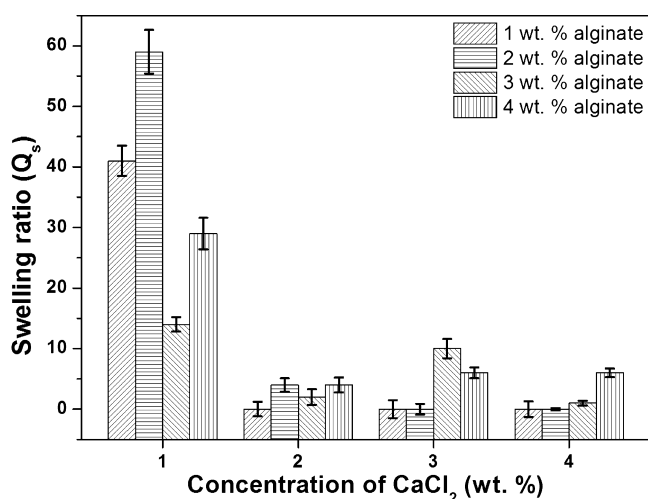


**Figure 3.** Optimization of the alginate and the  $\text{CaCl}_2$  solution concentration for the best swelling ratio.

largest swelling of the alginate hydrogel. To 9.4 mL of alginate solution at various concentrations (1, 2, 3, 4 wt %), 0.6 mL of  $\text{CaCl}_2$  solution at various concentrations (1, 2, 3, 4 wt %) was added. Within 30 s, an amorphous gel was formed. After 30 min of cross-linking reaction in the gel, any unbound calcium ions were washed off by deionized water several times. After drying the gel, in order to estimate how much swelling the gel can make, we measured the weight change of the hydrogel before and after immersing the dried gel into water (see Experimental Section for details about the calculation of the swelling ratio). Dried alginate gel began to swell within 1 min, and the swelling reached saturation in 1 h. When more than 1 wt %  $\text{CaCl}_2$  was used, the swelling ratio dropped down significantly (Figure 3) because large cross-linking density reduces the average molecular weight of the alginate segments between cross-linking points.<sup>45</sup> In contrast, at 1 wt %  $\text{CaCl}_2$ , regardless of alginate concentrations, the hydrogels showed distinctively higher swelling ratios. The best swelling ratio of about 60 was achieved from the gel prepared with a 2 wt % alginate solution (9.4 mL) and a 1 wt %  $\text{CaCl}_2$  solution (0.6 mL).

After establishing the gel formula, we incorporated 0.5 mM PCDA liposomes and 0.5 mM PCDA-IPA liposomes into the alginate hydrogel, respectively. 0.5 mM was a suitable concentration to make a discernible color transition when the liposomes are embedded in the alginate hydrogel. By cross-linking the liposomes and the alginate hydrogel with  $\text{Ca}^{2+}$ , we investigated how volumetric expansion of hydrated hydrogel affects the PDA mechanochromism. We could photopolymerize the embedded PDA liposomes to make blue hydrogel, confirming PDA liposomes are stable inside the hydrogel. Afterward, 1 mL of deionized water was added to a dried PDA-alginate hydrogel and the gel was kept at room temperature for 1 h. Through a systematic study considering a discernible PDA color transition in a hydrogel composite, the optimized concentration and volume of the hydrogel components (alginate, PDA liposome, and  $\text{CaCl}_2$  solution) were decided to make the highest contrast in the PDA color change. Dried blue PDA-alginate hydrogels swelled in water from  $\sim 6$  mm to  $\sim 10$  mm in diameter after 1 h (Figure 2c, d). However, we could not observe any noticeable chromism from the swollen

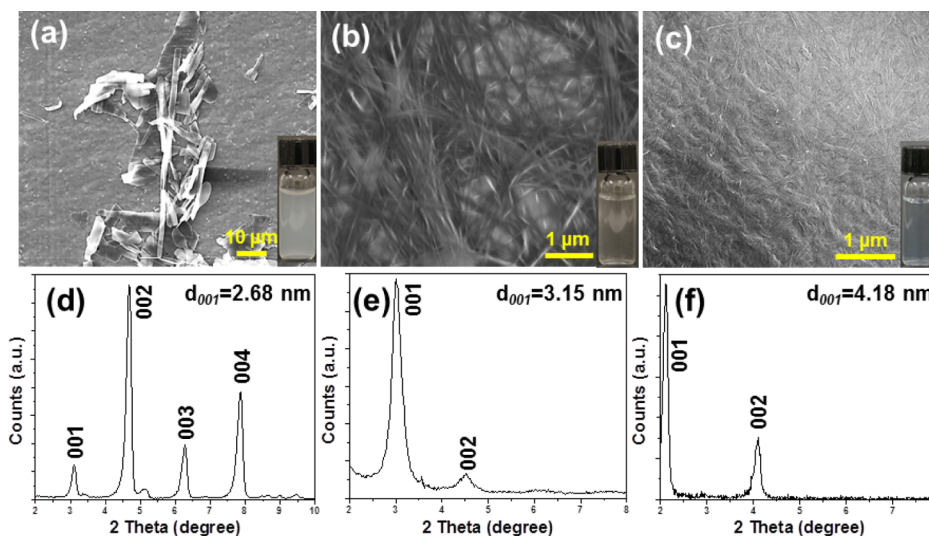


**Figure 4.** SEM images of (a) PCDA- $\text{Na}^+$  microcrystal, (b) PCDA-IPA- $\text{K}^+$  nanofiber, and (c) PCDA-IPA- $\text{Li}^+$  nanofiber. XRD patterns of (d) PCDA- $\text{Na}^+$  microcrystal, (e) PCDA-IPA- $\text{K}^+$  nanofiber, and (f) PCDA-IPA- $\text{Li}^+$  nanofiber.

gels with the naked eye as well as the colorimetric response (CR) from UV–vis absorption (see [Experimental Section](#) for details about CR calculation). As illustrated in [Figure 1a](#), we hypothesized that 0-dimensional liposomes cannot make

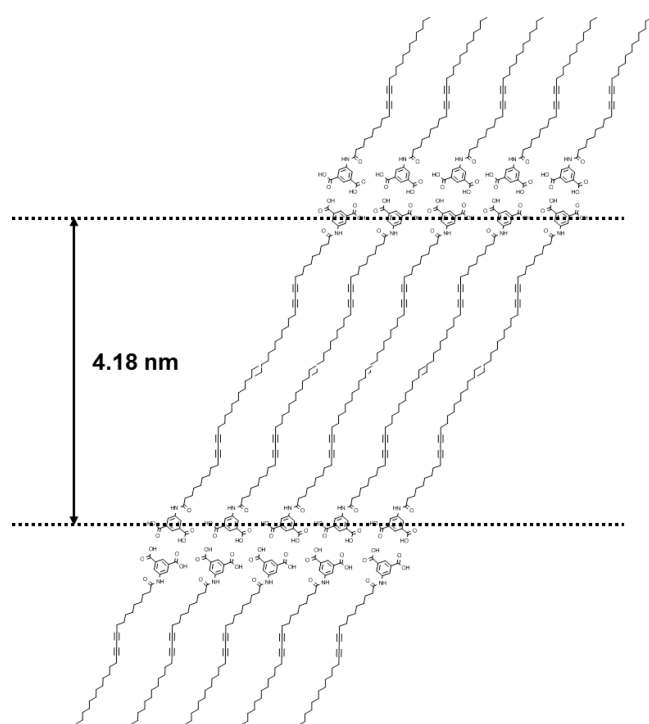


**Figure 5.** Proposed molecular packing structure of PCDA-IPA- $\text{Li}^+$  nanofiber.

enough cross-linking points with multiple alginate fibers in the gel so that swelling of the gel cannot efficiently impose stress on the embedded PDA liposomes to produce mechanochromism.

In order to examine whether a 1-dimensional PDA assembly, such as a microcrystal or nanofiber, is more advantageous by forming efficient multiple connection points with matrix alginate fibers than 0-dimensional PDA liposome, we prepared 1-dimensional PDA microcrystals and nanofibers. As shown in [Figure 4a–c](#), we prepared such a 1-dimensional assembly by using alkali metals: PCDA- $\text{Na}^+$  bulky microcrystals, PCDA-IPA- $\text{K}^+$  nanofiber having  $\sim 50$  nm diameter, and PCDA-IPA- $\text{Li}^+$  nanofiber with  $\sim 20$  nm diameter. Even though we do not fully understand the role of the alkali metals for the PDA nanostructure formation,  $\text{Li}^+$  produced the thinnest PCDA-IPA nanofiber. Photopolymerization of the 1-dimensional assemblies of PDA by a 254 nm UV lamp produced blue color, confirming that the diacetylene monomers are self-assembled into close and parallel packing. XRD analysis on these assemblies revealed a highly ordered lamellar structure ([Figure 4d–f](#)). The interlamellar distance calculated from the Bragg equation for PCDA- $\text{Na}^+$  bulky microcrystals, PCDA-IPA- $\text{K}^+$  nanofiber, and PCDA-IPA- $\text{Li}^+$  nanofiber was 2.68, 3.15, and 4.18 nm, respectively. This implies that the introduction of alkali metal ions promotes the formation of 1-dimensional structures by means of forming stronger intermolecular interactions, such as electrostatic interactions,<sup>48</sup>  $\pi$ – $\pi$  stacking, and hydrogen bonding between amide groups. Based on the XRD data, we proposed the highly ordered molecular packing structure of PCDA-IPA- $\text{Li}^+$  nanofibers depicted in [Figure 5](#).

The swelling ratio of the hydrogels with the embedded 1-dimensional PDA assemblies (PCDA- $\text{Na}^+$  microcrystal,

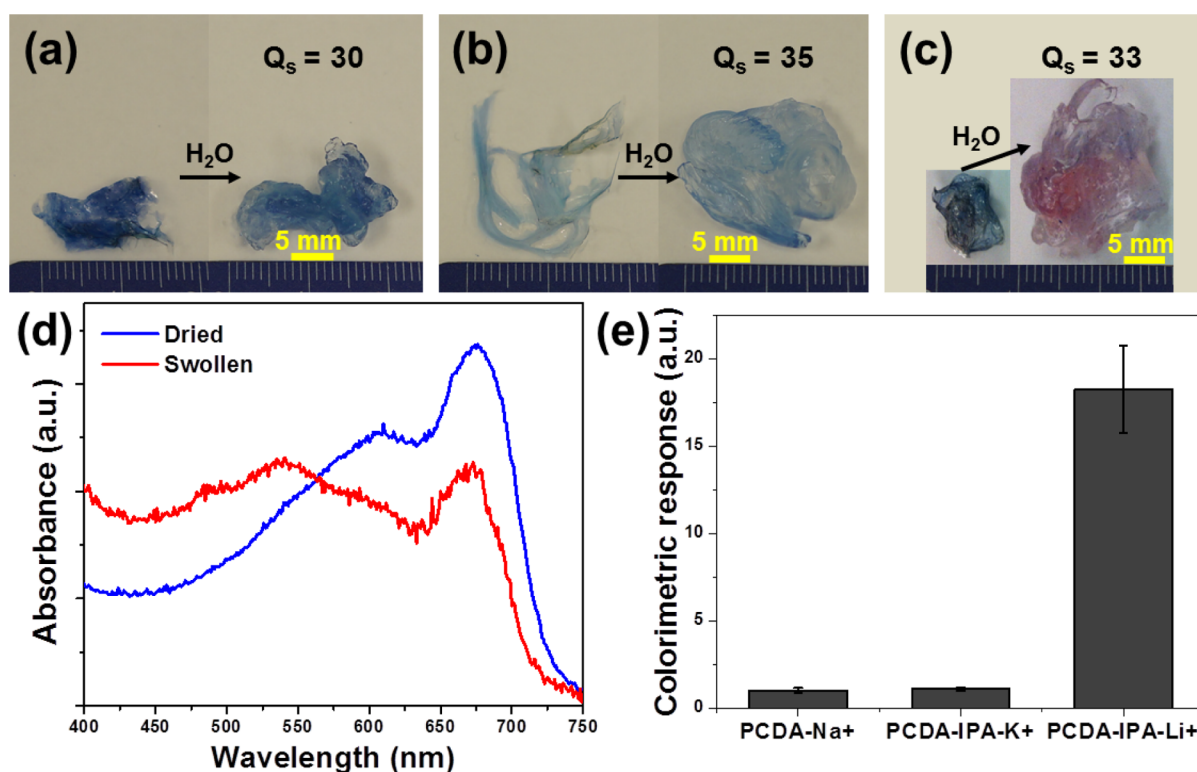


**Figure 6.** Photograph of photopolymerized/dehydrated alginate hydrogel and hydrated hydrogel embedded with (a) PCDA- $\text{Na}^+$  microcrystal, (b) PCDA-IPA- $\text{K}^+$  nanofiber, and (c) PCDA-IPA- $\text{Li}^+$  nanofiber. (d) UV–vis spectra of PCDA-IPA- $\text{Li}^+$  nanofiber-hydrogel in the dried and swollen state. (e) Colorimetric response of alginate hydrogels calculated from UV–vis absorption intensities.

PCDA-IPA-K<sup>+</sup> nanofiber, PCDA-IPA-Li<sup>+</sup> nanofiber) was in the range of 30–35 (Figure 6a–c). The swelling ratio is similar to the value of the PDA liposome incorporated hybrid system, expecting a comparable external volumetric change. Among the three 1-dimensional micro-/nanoassemblies, only the thinnest PCDA-IPA-Li<sup>+</sup> nanofiber hydrogel composite started to turn red within 1 min as the hydrogel began to swell, and the red color reached saturation in 1 h, which makes sense because it is likely that the thinner nanofiber is more sensitive to the same force exerted by swelling of the gel. As one can see from the UV–vis spectra in Figure 6d, we could confirm the red phase formation by the swelling. The colorimetric response of the hydrogel composites in this study was plotted in Figure 6e. The PCDA-IPA-Li<sup>+</sup> nanofiber hydrogel is most sensitive to the swelling of the hydrogel matrix. As shown in Figure 1, 1-dimensional fiber structures provide a larger surface area-to-volume ratio than 0-dimensional liposomes. Accordingly, 1-dimensional nanofibers would form more ionic cross-linking points with multiple alginate fibers to form an effective hydrogel network like the interpenetrating polymeric network between alginate and chitosan.<sup>45</sup> Moreover, the flexibility of nanofibers is compatible with the soft hydrogel matrix, and the gel swelling driven stress acts on the nanofibers efficiently, generating red color.

## CONCLUSIONS

We rationally combined PCDA-IPA nanofibers as a sensory unit and hygroscopic alginate polymers as a stimuli responsive matrix into a PDA nanofiber–alginate network in order to investigate stimuli-responsive matrix-driven colorimetric PDA sensory systems. Alginate is a hygroscopic biopolymer having a dramatic volume swelling property when it absorbs water. Various forms of self-assembled PDA were embedded into an alginate solution, and the mixture was cross-linked by calcium ions to form a gel. Zero-dimensional PDA liposomes unlikely make cross-linking points with multiple alginate fibers, and therefore, no colorimetric response was observed from the embedded PDA liposomes even after the alginate matrix largely swelled. Among the 1-dimensional PDA assemblies, the finest PDA nanofibers from the Li<sup>+</sup>-mediated self-assembly produced a sharp color change from blue to red when the coassembled and cross-linked alginate matrix polymer swelled by absorbing water, indicating that dimensionality is an important design factor to realize stimuli-responsive matrix-driven colorimetric PDA sensory systems. This design principle can be adapted for various optical sensor developments, for example, a temperature sensor utilizing volumetric expansion of thermoresponsive poly(*N*-isopropylacrylamide) (PNIPAm) as a matrix.

## AUTHOR INFORMATION

### Corresponding Author

\*E-mail: jinsang@umich.edu.

### Present Addresses

<sup>▽</sup>S. Seo: Marine Science Institute, University of California, Santa Barbara, California 93106, USA

<sup>○</sup>J. Lee: School of Energy and Chemical Engineering, Ulsan National Institute of Science and Technology (UNIST), Ulsan Metropolitan City 689-798, Republic of Korea

### Author Contributions

#S. Seo and J. Lee contributed equally.

### Notes

The authors declare no competing financial interest.

## ACKNOWLEDGMENTS

This study was supported by a grant from the Animal, Plant and Fisheries Quarantine and Inspection Agency of Korea (I-AD14-2011-13-11). This work was also partly supported by the Converging Research Center Program funded by the Ministry of Science, ICT and Future Planning (Project No. 2013K00314). S. Seo was also partly supported by a Fulbright scholarship.

## REFERENCES

- (1) Mateescu, A.; Wang, Y.; Dostalek, J.; Jonas, U. Thin Hydrogel Films for Optical Biosensor Applications. *Membranes* **2012**, *2*, 40–69.
- (2) Lee, K. Y.; Mooney, D. J. Hydrogels for Tissue Engineering. *Chem. Rev.* **2001**, *101*, 1869–1880.
- (3) Shoichet, M. S. Polymer Scaffolds for Biomaterials Applications. *Macromolecules* **2010**, *43*, 581–591.
- (4) Slaughter, B. V.; Khurshid, S. S.; Fisher, O. Z.; Khademhosseini, A.; Peppas, N. A. Hydrogels in Regenerative Medicine. *Adv. Mater.* **2009**, *21*, 3307–3329.
- (5) Tokarev, I.; Minko, S. Stimuli-Responsive Hydrogel Thin Films. *Soft Matter* **2009**, *5*, 511–524.
- (6) Hirokawa, Y.; Tanaka, T. Volume Phase Transition in a Nonionic Gel. *J. Chem. Phys.* **1984**, *81*, 6379–6380.
- (7) Jin, S.; Liu, M.; Zhang, F.; Chen, S.; Niu, A. Synthesis and Characterization of pH-Sensitivity Semi-IPN Hydrogel based on Hydrogen Bond between Poly(*N*-vinylpyrrolidone) and Poly(acrylic acid). *Polymer* **2006**, *47*, 1526–1532.
- (8) Elliott, J. E.; Macdonald, M.; Nie, J.; Bowman, C. N. Structure and Swelling of Poly(acrylic acid) Hydrogels: Effect of pH, Ionic Strength, and Dilution on the Crosslinked Polymer Structure. *Polymer* **2004**, *45*, 1503–1510.
- (9) Fujigaya, T.; Morimoto, T.; Niidome, Y.; Nakashima, N. NIR Laser-Driven Reversible Volume Phase Transition of Single-Walled Carbon Nanotube/Poly(*N*-isopropylacrylamide) Composite Gels. *Adv. Mater.* **2008**, *20*, 3610–3614.
- (10) Tanaka, T.; Nishio, I.; Sun, S.-T.; Ueno-Nishio, S. Collapse of Gels in an Electric Field. *Science* **1982**, *218*, 467–469.
- (11) Maitz, M. F.; Freudenberger, U.; Tsurkan, M. V.; Fischer, M.; Beyrich, T.; Werner, C. Bio-Responsive Polymer Hydrogels Homeostatically Regulate Blood Coagulation. *Nat. Commun.* **2013**, *4*, 2168.
- (12) Pan, L.; Yu, G.; Zhai, D.; Lee, H. R.; Zhao, W.; Liu, N.; Wang, H.; Tee, B. C.-K.; Shi, Y.; Cui, Y.; Bao, Z. Hierarchical Nanostructured Conducting Polymer Hydrogel with High Electrochemical Activity. *Proc. Natl. Acad. Sci. U. S. A.* **2012**, *109*, 9287–9292.
- (13) Xu, Y.; Sheng, K.; Li, C.; Shi, G. Self-Assembled Graphene Hydrogel via a One-Step Hydrothermal Process. *ACS Nano* **2010**, *4*, 4324–4330.
- (14) Sekine, S.; Ido, Y.; Miyake, T.; Nagamine, K.; Nishizawa, M. Conducting Polymer Electrodes Printed on Hydrogel. *J. Am. Chem. Soc.* **2010**, *132*, 13174–13175.
- (15) LaVan, D. A.; McGuire, T.; Langer, R. Small-Scale Systems for In Vivo Drug Delivery. *Nat. Biotechnol.* **2003**, *21*, 1184–1191.
- (16) Norton, L. W.; Tegnell, E.; Toporek, S. S.; Reichert, W. M. In Vitro Characterization of Vascular Endothelial Growth Factor and Dexamethasone Releasing Hydrogels for Implantable Probe Coatings. *Biomaterials* **2005**, *26*, 3285–3297.
- (17) Nakabayashi, N.; Williams, D. F. Preparation of Non-Thrombogenic Materials using 2-methacryloyloxyethyl phosphorylcholine. *Biomaterials* **2003**, *24*, 2431–2435.
- (18) Zhai, D.; Liu, B.; Shi, Y.; Pan, L.; Wang, Y.; Li, W.; Zhang, R.; Yu, G. Highly Sensitive Glucose Sensor Based on Pt Nanoparticle/Polyaniline Hydrogel Heterostructures. *ACS Nano* **2013**, *7*, 3540–3546.
- (19) Grigoryev, A.; Sa, V.; Gopishetty, V.; Tokarev, I.; Kornev, K. G.; Minko, S. Wet-Spun Stimuli-Responsive Composite Fibers with Tunable Electrical Conductivity. *Adv. Funct. Mater.* **2013**, *23*, 5903–5909.

- (20) Ramesh, G. V.; Radhakrishnan, T. P. A Universal Sensor for Mercury (Hg, Hg<sup>I</sup>, Hg<sup>II</sup>) Based on Silver Nanoparticle-Embedded Polymer Thin Film. *ACS Appl. Mater. Interfaces* **2011**, *3*, 988–994.
- (21) Kim, E.; Kim, S. Y.; Jo, G.; Kim, S.; Park, M. J. Colorimetric and Resistive Polymer Electrolyte Thin Films for Real-time Humidity Sensors. *ACS Appl. Mater. Interfaces* **2012**, *4*, 5179–5187.
- (22) Ferhan, A. R.; Guo, L.; Zhou, X.; Chen, P.; Hong, S.; Kim, D.-H. Solid-Phase Colorimetric Sensor Based on Gold Nanoparticle-Loaded Polymer Brushes: Lead Detection as a Case Study. *Anal. Chem.* **2013**, *85*, 4094–4099.
- (23) Carpick, R. W.; Sasaki, D. Y.; Burns, A. R. First Observation of Mechanochromism at the Nanometer Scale. *Langmuir* **2000**, *16*, 1270–1278.
- (24) Ryu, S.; Yoo, I.; Song, S.; Yoon, B.; Kim, J.-M. A Thermoresponsive Fluorogenic Conjugated Polymer for a Temperature Sensor in Microfluidic Devices. *J. Am. Chem. Soc.* **2009**, *131*, 3800–3801.
- (25) Cheng, Q.; Stevens, R. C. Charge-Induced Chromatic Transition of Amino Acid-Derivatized Polydiacetylene Liposomes. *Langmuir* **1998**, *14*, 1974–1976.
- (26) Jonas, U.; Shah, K.; Norvez, S.; Charych, D. H. Reversible Color Switching and Unusual Solution Polymerization of Hydrazide-Modified Diacetylene Lipids. *J. Am. Chem. Soc.* **1999**, *121*, 4580–4588.
- (27) Tomioka, Y.; Tanaka, N.; Imazeki, S. Effects of Side-Group Interactions on Pressure-Induced Chromism of Polydiacetylene Monolayer at a Gas-Water Interface. *Thin Solid Films* **1989**, *179*, 27–31.
- (28) Tashiro, K.; Nishimura, H.; Kobayashi, M. First Success in Direct Analysis of Microscopic Deformation Mechanism of Polydiacetylene Single Crystal by the X-ray Imaging-Plate System. *Macromolecules* **1996**, *29*, 8188–8196.
- (29) Seo, S.; Lee, J.; Choi, E.-J.; Kim, E.-J.; Song, J.-Y.; Kim, J. Polydiacetylene Liposome Microarray Toward Influenza A Virus Detection: Effect of Target Size on Turn-On Signaling. *Macromol. Rapid Commun.* **2013**, *34*, 743–748.
- (30) Kang, D. H.; Jung, H.-S.; Ahn, N.; Lee, J.; Seo, S.; Suh, K.-Y.; Kim, J.; Kim, K. Biomimetic Detection of Aminoglycosidic Antibiotics using Polydiacetylene-Phospholipids Supramolecules. *Chem. Commun.* **2012**, *48*, 5313–5315.
- (31) Lee, J.; Seo, S.; Kim, J. Colorimetric Detection of Warfare Gases by Polydiacetylenes Toward Equipment-Free Detection. *Adv. Funct. Mater.* **2012**, *22*, 1632–1638.
- (32) Lee, J.; Jeong Jeong, E.; Kim, J. Selective and Sensitive Detection of Melamine by Intra/Inter Liposomal Interaction of Polydiacetylene Liposomes. *Chem. Commun.* **2011**, *47*, 358–360.
- (33) Lee, J.; Jun, H.; Kim, J. Polydiacetylene–Liposome Microarrays for Selective and Sensitive Mercury(II) Detection. *Adv. Mater.* **2009**, *21*, 3674–3677.
- (34) Lee, J.; Kim, H.-J.; Kim, J. Polydiacetylene Liposome Arrays for Selective Potassium Detection. *J. Am. Chem. Soc.* **2008**, *130*, 5010–5011.
- (35) Seo, D.; Kim, J. Effect of the Molecular Size of Analytes on Polydiacetylene Chromism. *Adv. Funct. Mater.* **2010**, *20*, 1397–1403.
- (36) Chen, X.; Kang, S.; Kim, M. J.; Kim, J.; Kim, Y. S.; Kim, H.; Chi, B.; Kim, S.-J.; Lee, J. Y.; Yoon, J. Thin-Film Formation of Imidazolium-Based Conjugated Polydiacetylenes and Their Application for Sensing Anionic Surfactants. *Angew. Chem., Int. Ed.* **2010**, *49*, 1422–1425.
- (37) Charych, D.; Nagy, J.; Spevak, W.; Bednarski, M. Direct Colorimetric Detection of a Receptor-Ligand Interaction by a Polymerized Bilayer Assembly. *Science* **1993**, *261*, 585–588.
- (38) Kolusheva, S.; Kafri, R.; Katz, M.; Jelinek, R. Rapid Colorimetric Detection of Antibody–Epitope Recognition at a Biomimetic Membrane Interface. *J. Am. Chem. Soc.* **2001**, *123*, 417–422.
- (39) Lee, J.; Chang, H. T.; An, H.; Ahn, S.; Shim, J.; Kim, J.-M. A Protective Layer Approach to Solvatochromic Sensors. *Nat. Commun.* **2013**, *4*, 2461.
- (40) Park, D.-H.; Hong, J.; Park, I. S.; Lee, C. W.; Kim, J.-M. A Colorimetric Hydrocarbon Sensor Employing a Swelling-Induced Mechanochromic Polydiacetylene. *Adv. Funct. Mater.* **2014**, *24*, 5186–5193.
- (41) Lee, J.; Balakrishnan, S.; Cho, J.; Jeon, S.-H.; Kim, J.-M. Detection of Adulterated Gasoline using Colorimetric Organic Microfibers. *J. Mater. Chem.* **2011**, *21*, 2648–2655.
- (42) Lee, J.; Pyo, M.; Lee, S.-h.; Kim, J.; Ra, M.; Kim, W.-Y.; Park, B. J.; Lee, C. W.; Kim, J.-M. Hydrochromic Conjugated Polymers for Human Sweat Pore Mapping. *Nat. Commun.* **2014**, *5*, 3736.
- (43) Lee, J.-S.; Lee, S.; Kim, J.-M. Fluorogenic Conjugated Polymer Fibers from Amphiphilic Diacetylene Supramolecules. *Macromol. Res.* **2008**, *16*, 73–75.
- (44) Bai, F.; Sun, Z.; Lu, P.; Fan, H. Smart Polydiacetylene Nanowire Paper with Tunable Colorimetric Response. *J. Mater. Chem.* **2012**, *22*, 14839–14842.
- (45) Lin, Y.-H.; Liang, H.-F.; Chung, C.-K.; Chen, M.-C.; Sung, H.-W. Physically Crosslinked Alginate/N,O-carboxymethyl Chitosan Hydrogels with Calcium for Oral Delivery of Protein Drugs. *Biomaterials* **2005**, *26*, 2105–2113.
- (46) Okada, S.; Peng, S.; Spevak, W.; Charych, D. Color and Chromism of Polydiacetylene Vesicles. *Acc. Chem. Res.* **1998**, *31*, 229–239.
- (47) Rowe, R. C.; Sheskey, P. J.; Quinn, M. E. *Handbook of Pharmaceutical Excipients*, 6th ed.; Royal Pharmaceutical Society: U.K., 2009.
- (48) Pang, J.; Yang, L.; McCaughey, B. F.; Peng, H.; Ashbaugh, H. S.; Brinker, C. J.; Lu, Y. Thermo-chromatism and Structural Evolution of Metastable Polydiacetylenic Crystals. *J. Phys. Chem. B* **2006**, *110*, 7221–7225.